MAGNETIC RESONANCE IN CHEMISTRY
Magn. Reson. Chem. 2001; **39**: S81–S90

Dimerization and solvent-assisted proton dislocation in the low-barrier hydrogen bond of a Mannich base: a low-temperature NMR study

Maria Rospenk,[1] Lucjan Sobczyk,[1] Parwin Schah-Mohammedi,[2] Hans-Heinrich Limbach,[2]* Nicolai S. Golubev[3] and Sonya M. Melikova[3]

[1] Faculty of Chemistry, University of Wrocław, Joliot-Curie 14, 50-383 Wrocław, Poland
[2] Institut für Chemie, Freie Universität Berlin, Takustrasse 3, D-14195 Berlin, Germany
[3] Institute of Physics, St. Petersburg State University, 198-904 St. Petersburg, Russia

Received 15 April 2001; Revised 23 August 2001; Accepted 24 August 2001

Using low-temperature UV, ^{1}H and ^{15}N NMR spectroscopy, we studied the easily polarizable O—H···N↔O$^{\delta-}$···H···N$^{\delta+}$ ↔O$^-$···H—N$^+$ hydrogen bond of the labeled Mannich base[^{15}N] 2-(*N*,*N*-diethylaminomethyl)-3,4,6-trichlorophenol (Cl_3MB) dissolved in dichloromethane and in a 2:1 mixture of CDF_3 and $CDClF_2$. Whereas at high temperature the molecule is present as a monomer exhibiting an intramolecular hydrogen bond, at low temperature two different cyclic hydrogen-bonded dimers are formed which have been observed for the first time by NMR in the slow hydrogen bond exchange regime. The proton chemical shifts and the scalar ^{1}H, ^{15}N coupling constants indicate a quasi-symmetric low-barrier hydrogen bond in the monomer but polar O$^-$···H—N$^+$ hydrogen bonds exhibiting a considerable charge separation in the case of the dimers. The thermodynamics of the association process were elucidated by UV and NMR spectroscopy. Interestingly, it was found that the addition of methanol does not change substantially the monomer–dimer equilibrium but leads to a considerable shift of the proton in the monomer towards the nitrogen atom. The effect is smaller but also observable for the dimers. In order to assign molecular structures to the observed species, DFT calculations were performed. They reveal a variety of both monomeric and dimeric conformations of Cl_3MB exhibiting different hydrogen bond geometries. In particular, two monomeric conformations, bent and planar, were found which exhibit almost the same energy and two proton-transfer dimeric species of similar energy and different dipole moments. **Copyright © 2001 John Wiley & Sons, Ltd.**

KEYWORDS: ^{1}H NMR; ^{15}N NMR; Mannich base; hydrogen bond; low-temperature NMR; dimerization; proton dislocation

INTRODUCTION

Mannich bases (Scheme 1) exhibit interesting hydrogen bond properties which have been studied using a number of spectroscopic techniques.[1–20] In aprotic solvents these molecules normally exist as molecular monomers M exhibiting an intramolecular O—H···N hydrogen bond [Scheme 1(a)]. The hydrogen bond does not even break in the gas phase at elevated temperatures.[4]

The hydrogen bond geometry and especially the average proton position can be manipulated by varying the substituents of the phenyl ring [1–3] via an enhancement of the acidity of the OH group. This acidity increase induces a very strong red shift of the long-wavelength ^1L_b electronic absorption band of the phenyl group[5] which depends in a very sensitive way on the substituents and solvents used.[6–12] The observation of broad 'continuous' absorption bands[13,14] in the infrared spectra of Mannich bases[13,14] indicated that the intramolecular hydrogen bond is very strong, i.e. of the low-barrier hydrogen bond type as depicted in Scheme 1(b). For example, the NMR spectra of Mannich bases exhibit hydrogen bond proton signals at low field;[15–17] furthermore, interesting temperature-dependent H/D isotope effects on ^{13}C chemical shifts have been observed.[18] As the x-ray diffraction of Mannich bases[3] does not lead to conclusive results concerning the proton location, many efforts have been made to solve the following problem: are Mannich bases characterized by a conventional proton transfer equilibrium between two limiting forms, i.e. a nonpolar form [Scheme 1(a)] and a zwitterionic form [Scheme 1(c)] where the proton transfer involves an energy barrier, or does the proton always move in a single well potential, but where the minimum of the potential is gradually shifted from oxygen when the acidity of the OH group is increased, passing a quasi-symmetric structure of the type as indicated in Scheme 1(b)?

*Correspondence to: H.-H. Limbach, Institute für Chemie, Freie Universität Berlin, Takustrasse 3, D-14195 Berlin, Germany.
Contract/grant sponsor: Deutsche Forschungsgemeinschaft.
Contract/grant sponsor: Fonds der Chemischen Industrie.
Contract/grant sponsor: Polish Committee for Scientific Research;
Contract/grant number: 09A03416.

DOI: 10.1002/mrc.943

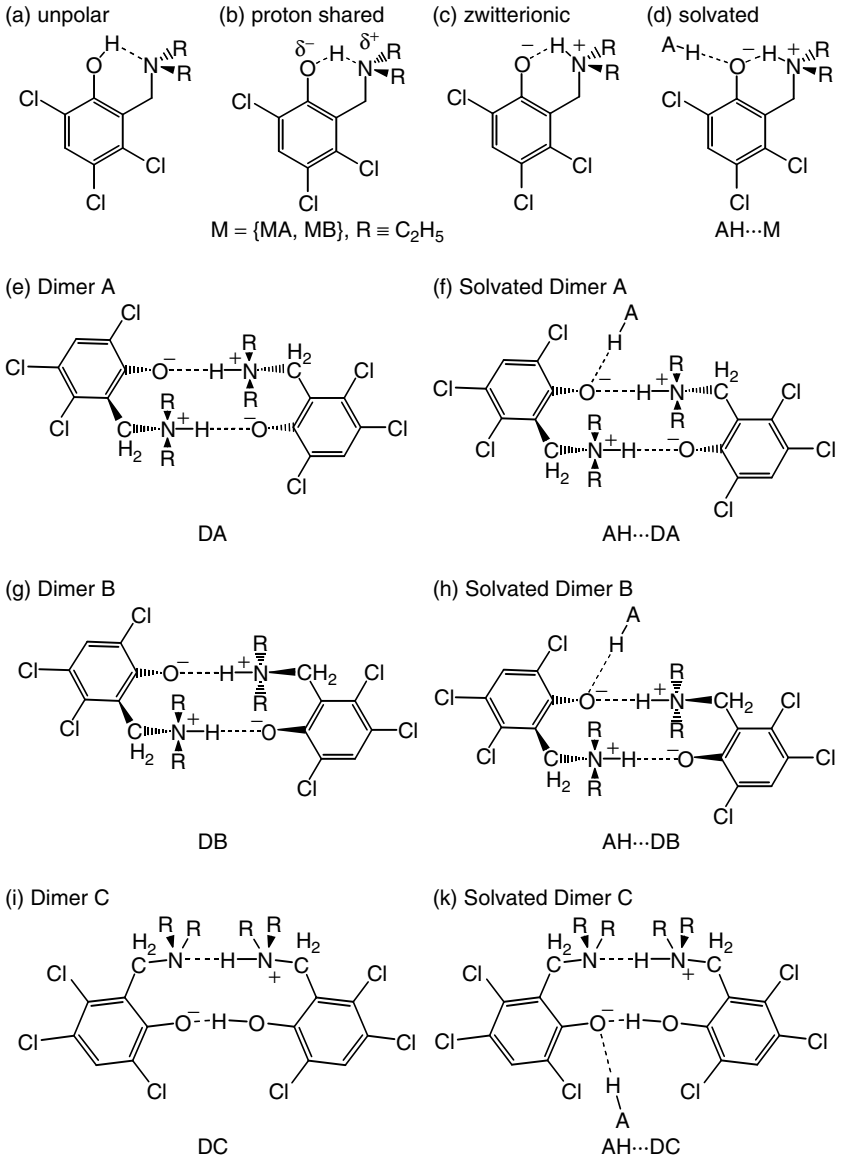

Scheme 1. Structures of the Mannich base **1**, [^{15}N]-2-(diethylaminomethyl)-3,4,6-trichlorophenol (Cl_3MB), under different conditions.

Although arguments can be found for both proton transfer mechanisms, the interpretation of the spectroscopic results is most often complicated by a variety of intramolecular and intermolecular changes. For example, the flexibility of the Mannich bases may lead to different conformers exhibiting so far unknown structures and hence different H-bond geometries, e.g. MA and MB [Scheme 1(a)–1(c)]. Moreover, especially intermolecular interactions can alter the hydrogen bond geometry. For example, dipole moment measurements[19] and UV spectroscopic and molecular weight studies[20] have provided evidence for the formation of unsymmetrical dimers D exhibiting large dipole moments, where the proton is closer to nitrogen than to oxygen. These polar dimers have the tendency to form higher associates in solvents of low polarity.[20] As indicated in Scheme 1, one can conceive various structures such as DA and DB exhibiting both two O···H···N hydrogen bonds, which are distinguished by a different conformation of the substituents R on nitrogen, and a symmetric dimer DC exhibiting homoconjugated O···H···O^- and N···H···N^+ hydrogen bonds. Zwitterionic hydrogen bond structures of the monomer and the dimers may also be formed by adding proton donors such as methanol as indicated in Scheme 1. However, little is known about either the structure of these solvated monomers or the structure of the cyclic dimers.

The scope of the present study was, therefore, to study the above-mentioned problems by a combined strategy. First, this strategy involves low-temperature NMR measurements using a liquefied mixture of CDF_3–CDF_2Cl (2 : 1) in order to reach the slow hydrogen bond exchange regime[21,22] necessary to distinguish monomers and dimers. Moreover, the dielectric constant of this solvent is strongly increased when the temperature is lowered. The dielectric constant of CHF_3–CHF_2Cl (1 : 1) increases from about 20 at 170 K to 45 at 95 K.[23] In addition, we chose to synthesize and study a ^{15}N-labeled Mannich base, [^{15}N]-2-(diethylaminomethyl)-3,4,6-trichlorophenol (Cl_3MB) as a model compound (Scheme 1), in order to take advantage of scalar couplings $^1J(^1H,^{15}N)$ between the hydrogen bond proton and nitrogen for obtaining structural information about the hydrogen bond

geometry. Second, we performed UV experiments under similar experimental conditions as chosen for the NMR experiments. Third, we performed DFT calculations of the various monomeric and dimeric structures of Scheme 1 in order to obtain an idea of the possible conformations of these species.

We first describe details of the synthesis and the experiments and the calculations performed. Then we describe the results of our measurements performed on Cl_3MB dissolved in CDF_3–CDF_2Cl (2 : 1), with and without the presence of methanol, and the results of the calculations. Finally, all results are discussed in terms of an acidity increase of the OH group of the title compound associated with a proton shift from oxygen to nitrogen, induced at low temperatures by (i) the increased solvent polarity, (ii) the dimerization and (iii) solvation by methanol molecules.

EXPERIMENTAL

Cl_3MB labeled with ^{15}N was synthesized from 2,4,5-trichlorophenol and [^{15}N]diethylamine according to a procedure described for the non-labeled material[24].

The Freon mixture CDF_3–$CDClF_2$ (2 : 1) was prepared as described previously at 100 °C and pressures up to 40 bar.[22,25] The solvent was handled on a high vacuum line which was also used to prepare the samples. The substance was placed in a special thick-walled sample tube (Spintec) with a PTFE valve. The NMR spectra were measured on a Bruker AMX 500 spectrometer. The overall concentrations of the sample were determined by weighing.

The low-temperature UV spectra were recorded using a Cary 1 UV–VIS spectrophotometer equipped with a laboratory-built cryostat.

Analysis of thermodynamic and kinetic data

In order to analyze the thermodynamic and kinetic data for the dimerization of Mannich bases in polar aprotic media, we assumed in a first stage the reaction network of Scheme 2(a), which includes two dimers DA and DB, as found later experimentally.

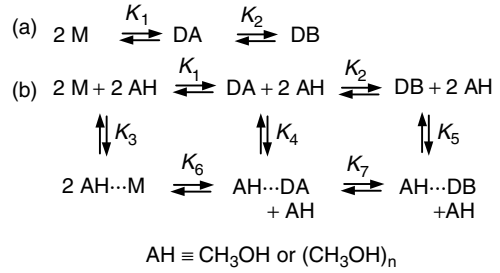

Scheme 2. Dimerization and solvation models of the Mannich base **1** in Freon solution.

The equilibrium constants of the association reaction of Scheme 2(a) are given by

$$K_1 = c_{DA}/c_M^2,\ K_2 = c_{DB}/c_{DA} \tag{1}$$

where c_{DA}, c_{DB} and c_M represent the concentrations of dimer A, dimer B and the monomer M, respectively, with the total concentration of the solute given by

$$C_X = c_M + 2c_{DA} + 2c_{DA} \tag{2}$$

If I_{DA}, I_{DB} and I_M are the corresponding integrated signal intensities, and $I_D = I_{DA} + I_{DB}$, it follows that

$$K_1 = I_M/I_D(I_M/I_D + 1)/[2(1 + I_{DB}/I_{DA})C_X],\ K_2 = I_{DB}/I_{DA} \tag{3}$$

In the case of UV spectroscopy, the two dimers were not resolved. In this case only the constant

$$K_D = c_D/c_M^2 = (c_{DA} + c_{DB})/c_M^2 = K_1(1 + K_2) \tag{4}$$

could be observed.

In the presence of methanol, both the monomer and the dimers are solvated by methanol molecules. The structure of these associates is not known, and detailed thermodynamic data could not be obtained. Although we are aware that this is a crude approximation, we treated the solvation of M, DA and DB as independent of each other. Moreover, we replaced the methanol clusters $(CH_3OH)_n$ with an unknown number n by a single proton donor AH. These assumptions allow us to simplify the complicated equilibrium of Scheme 2(b) to the simpler scheme

$$AH + X \underset{k_b}{\overset{k_f}{\rightleftharpoons}} AH\cdots X,\ K = k_f/k_b = c_{AHX}/c_{AH}c_X \tag{5}$$

This equation will be used for all cases, i.e. X = M, DA and DB. K can be determined in each case from the chemical shifts and taken as rough for K_3, K_4 and K_5 in Scheme 2(b) as follows. In the fast solvation exchange regime the chemical shifts of X are averages over the solvated and the non-solvated forms. For this case it has been shown [26] that

$$\delta = \delta(X) + [\delta(AH\cdots X) - \delta(X)]c_{AHX}/C_X \tag{6}$$

with

$$\begin{aligned} x_{AHX} &= c_{AHX}/C_X \\ &= \left[-\sqrt{[(C_XK)^{-2} + (1-R)^2 + 2(C_XK)^{-1}(1+R)]}\right. \\ &\quad \left.+(C_XK)^{-1} + 1 + R\right]/2 \end{aligned} \tag{7}$$

where R is the molar equivalent of AH with respect to the total concentration C_X of X and $\delta(X)$ and $\delta(AH\cdots X)$ are the intrinsic limiting chemical shifts of the non-solvated and solvated forms. By plotting δ as a function of R it is possible to obtain both the intrinsic chemical shifts and K.

Finally, an estimate of the solvation kinetics can be obtained from lineshape simulations of the species in Eqn (5). By NMR, only the inverse lifetimes or the pseudo-first-order rate constants in hertz are obtained. If k_f is the forward rate constant for the 'solvation' process and k_b the corresponding rate constant for the backward reaction, the inverse lifetime of $AH\cdots X$ is

$$k_b' = k_b \tag{8}$$

The inverse lifetime of X is calculated from

$$k'_f = k_f c_{AH}, \text{ with } K' = k'_f/k_b = c_{AHX}/c_X = x_{AHX}/x_X = Kc_{AH} \quad (9)$$

Below, we will set $k'_f = k_{12}$, $k_b = k_{21}$, $x_X = x_1$ and $x_{AHX} = x_2$ in order to simplify the notation.

RESULTS

UV spectroscopy of Cl_3MB

In Figure 1(a) is depicted the room temperature UV spectrum of Cl_3MB dissolved in dichloromethane. For comparison, we include the spectrum of the *O*-methylated compound $MOCH_3$ obtained under the same conditions. Whereas the latter gives rise to a broad ^1L_b absorption band around 290 nm, the corresponding band of Cl_3MB is (i) enhanced and (ii) red shifted to about 300 nm. Further interesting changes occur when spectra are taken at low temperatures using CHF_3–$CHClF_2$ (2 : 1) as solvent [Fig. 1(b)]. Gradually a new band appears around 320 nm whose integrated intensity increases as the temperature is lowered and as the concentration is raised. Therefore, we assign this new band to a dimeric structure D. The temperature dependence of the integrated intensity of the band at about 320 nm was used to determine the equilibrium constant K_D of the formation of the dimers according to Eqn (4). From the temperature dependence of K_D in the range between 160 and 100 K we estimate the average dimerization enthalpy $\Delta H^o = -9.3 \pm 0.5$ kJ mol^{-1} and entropy $\Delta S^o = -16.8 \pm 2.2$ J K^{-1} mol^{-1}. The results are given in Table 1 and depicted in Fig. 1(c) as a van't Hoff plot. In the plot the data obtained from NMR at $c = 1.5 \times 10^{-3}$ M are included. Good agreement between the UV and NMR results should be noted.

^1H and ^{15}N NMR spectroscopy of Cl_3MB

The evolution of the experimental and calculated hydrogen bond proton signals of Cl_3MB obtained in the temperature range 150–110 K using CDF_3–$CDClF_2$ (2 : 1) as solvent are depicted in Fig. 2(a). The spectra consist of two groups of signals, one around 17 ppm and the other around 12 ppm. The ratio of the intensities for the two signals depends strongly on temperature. On lowering the temperature or increasing the concentration (unfortunately quantitative studies of concentration effects on NMR spectra were not possible owing to limited solubility at low temperatures), the intensity of the high-field signal rapidly grows which can, therefore, be assigned to the dimeric Mannich base. The signal consists, however, of two doublets of different intensities characterized by coupling constants $^1J(^1H, ^{15}N)$ of 67 and 70 Hz, which may therefore be assigned to two dimers with different conformations, e.g. DA and DB. Structure DC is excluded as in this case two hydrogen bond proton signals with different chemical shifts should be observed, one exhibiting a triplet structure by coupling with two ^{15}N atoms.

At 120 K the low-field signal exhibits a doublet splitting which we assign to scalar coupling with ^{15}N, where the coupling constant of $^1J(^1H, ^{15}N)$ is ~40 Hz. This much smaller value is consistent with a proton between oxygen or nitrogen, or jumping between these atoms. At the lowest temperature the low-field signal exhibits a decoalescence into a smaller, broader low-field component and a sharper

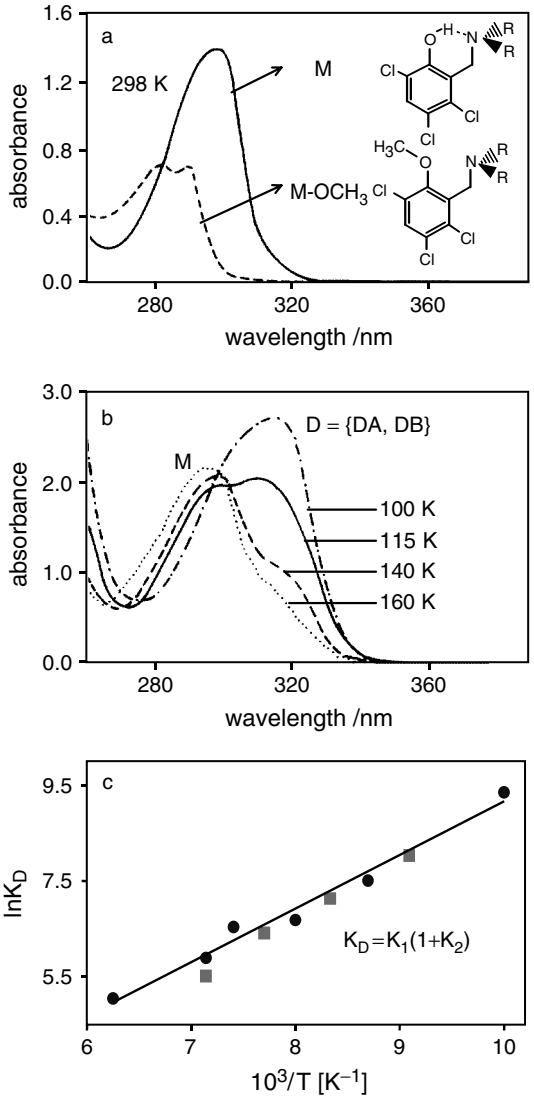

Figure 1. UV spectra of (a) Cl_3MB (**1**) and *O*-methylated Cl_3MB (**2**) in dichloromethane at room temperature. Concentration $C = 4 \times 10^{-4}$ M, cell pathlength $d = 1$ cm and (b) Cl_3MB in CHF_3–$CHClF_2$ (2 : 1) as a function of temperature ($C = 4 \times 10^4$ M, $d = 1.5$ cm). (c) Van't Hoff plot for Cl_3MB in Freons over the temperature range 100–160 K; squares correspond to data obtained from NMR at $C = 1.5 \times 10^{-3}$ M.

Table 1. Equilibrium constant $K_D = K_1(1 + K_2)$ for the dimerization of the Mannich base Cl_3MB in CHF_3–$CHClF_2$ (2 : 1) as a function of temperature

T(K)	K_D(l mol^{-1})	ΔH^o (kJ mol^{-1})	$-\Delta S^o$(J mol^{-1})	$-\Delta G^o$ (kJ mol^{-1})
100	11.42×10^3		15.3	7.77
115	1.81×10^3		18.5	7.17
125	7.96×10^2	-9.3 ± 0.5	18.9	6.94
135	6.83×10^2		14.3	7.33
140	3.63×10^2		17.4	6.86
160	1.54×10^2		16.3	6.70

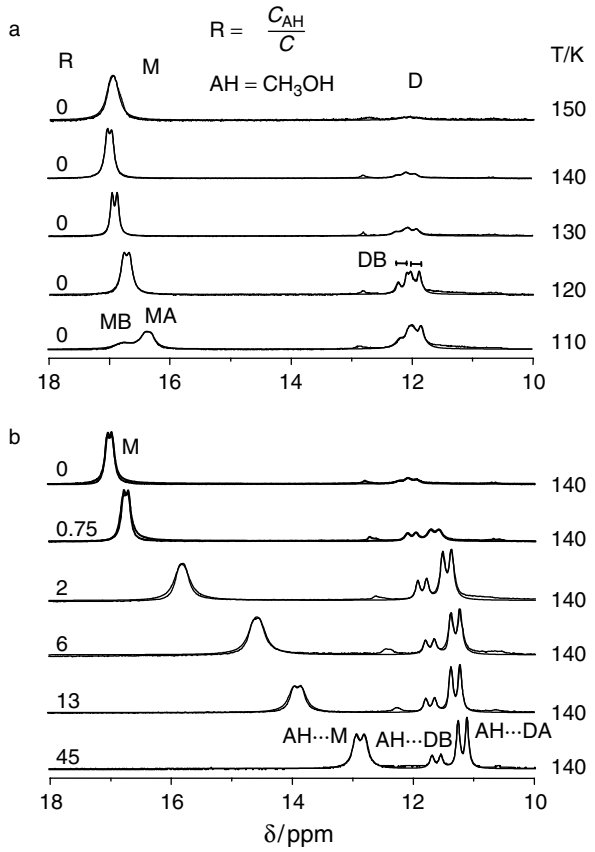

Figure 2. (a) Superposed experimental and calculated ^{1}H NMR signals of the hydrogen bond protons of Cl_3MB dissolved in of CDF_3–$CDClF_2$ (2 : 1). (a) at a total concentration $C = 1.5 \times 10^{-3}$ M. (b) Spectra obtained at 140 K at a concentration $C = 1.5 \times 10^{-3}$ M as a function of added equivalents R of methanol.

high-field component, preventing the determination of the coupling constants. We assign the two signals to two fast-exchanging monomers M exhibiting slightly different conformations. At high temperatures coupling constants could not be determined because of the onset of hydrogen bonding and proton exchange.

Chemical shifts, coupling constants, intrinsic linewidths and intensities are slightly dependent on temperature. All spectral parameters were determined by simulation of the spectra, and the results are given in Table 2.

In spite of the fact that the chemical shifts of sp^3 nitrogen atoms are much less sensitive to the nitrogen–hydrogen distance, we measured some low-temperature ^{15}N NMR spectra of the sample corresponding to Fig. 2(a). We observe at 120 K two broad signals around 19.5 and 34.0 ppm with respect to ammonium chloride. We assign the high-field line to the monomer M and the low-field line, which unfortunately was not resolved, to the dimers DA and DB. The chemical shift difference between the two signals probably arises not from the dimerization process but from the associated proton shift towards nitrogen, as manifest in the increase in the scalar coupling constant $^1J(^1H, ^{15}N)$ mentioned above. The two dimer ^{15}N resonances should be slightly different, but the transverse relaxation times are too short to resolve this difference.

The signal intensity ratios determined by lineshape analysis, listed in Table 2, give information about the thermodynamics of the dimerization process, which was interpreted in terms of the equilibria of Eqn (2). Using Eqns (3) and (4), the intensity ratios listed in Table 2 can be converted into the values of K_1. In view of the small temperature window and scattering of experimental data available, we were not able to determine the reaction enthalpies and entropies for the two steps in Eqn (2) with sufficient accuracy.

As we were interested in elucidating the influence of the increasing solvent activity on the monomer–dimer equilibrium, we prepared samples of the Mannich base ($C \approx 10^{-3}$ mol l^{-1}) with different equivalents R of methanol added. A series of spectra obtained at 140 K as a function of R are depicted in Fig. 2(b). We observe a monotonous shift of the monomer signal to high field in the range from 17 to 13 ppm. This finding can be explained by the H bond donor property of methanol, which forms additional hydrogen bonds with the negatively charged oxygen atom of the Mannich base [AH···M in Scheme 1(d)]. The analysis based on Eqns (5)–(9) enabled us to estimate the proton chemical shifts for the complexes of given species with methanol. They correspond to the threshold values of the solvated monomers [Fig. 3(a)] and the dimers DA [Fig. 3(b)] and DB [Fig. 3(c)] and are equal to 12.35, 11.6 and 11.18 ppm, respectively. The kinetic parameters obtained by line shape analysis are assembled in Table 3.

DISCUSSION

We have studied using UV and low-temperature liquid-state NMR the hydrogen bond properties of the Mannich base Cl_3MB dissolved in polar organic solvents. The UV spectra indicate two forms, where the equilibrium constants were determined from the integrated band intensities. As corroborated by NMR, we assign the two bands to the monomer M and the dimer D. M exhibits a large red shift of the ^1L_b absorption band as compared with the derivative where the intramolecular hydrogen bond is suppressed by replacement of the hydrogen bond proton by a methyl group. This red shift is consistent with a hydrogen bond geometry where a proton is shared between oxygen and nitrogen. A further red shift occurs in the dimer, showing a further proton dislocation towards nitrogen.

For the first time, we were able to observe the dimerization process also by NMR in the slow hydrogen bond exchange regime. Here, we observe also the monomer M but two different dimers DA and DB in the slow hydrogen bond exchange regime. The monomer is characterized by a low-field NMR chemical shift for the hydrogen bond proton around 17 ppm and a relatively small coupling constant $^1J(^1H, ^{15}N)$ of about 40 Hz which corroborates the strong intramolecular low-barrier hydrogen bond, with a proton shared between oxygen and nitrogen ($O^{\delta-}\cdots H\cdots N^{\delta+}$), although a very fast equilibrium between non-polar and a zwitterionic tautomer exhibiting the limiting structures of Scheme 1(a) and (c), populated to similar extents, cannot be excluded. Hence, the problem of the potential for the proton motion in M remains open.

Table 2. NMR parameters of Cl_3MB dissolved in CDF_3–CDF_2Cl (2 : 1), $C = 1.5 \times 10^{-3}$ M, in the absence and presence of methanol

					J[N,H(MA)]								J[N,H(DA)]					J[N,H(DB)]		
R	TK)	δ^1H_{MA}	W_{MA}	I_{MA}	(Hz)	δ^1H_{MB}	W_{MB}	I_{MB}	δ^1H_{DA}	W_{DA1}	W_{DA2}	I_{DA}	(Hz)	δ^1H_{DB}	W_{DB1}	W_{DB2}	I_{DB}	(Hz)	I_D/I_M	$I_{DB}/I_{DA} = K_2$
0	150	17.05	90	1	40	—	—	—	—	—	—	—	—	—	—	—	—	—	—	—
0	140	16.98	47	0.83	40	—	—	—	12.17	63	65	0.06	71	12.01	66	64	0.11	68	0.21	1.83
0	130	16.92	35	0.7	42	—	—	—	12.19	84	77	0.11	71	11.99	75	71	0.19	72	0.43	1.73
0	120	16.73	61	0.58	45	—	—	—	12.17	47	36	0.15	72	11.96	52	46	0.27	70	0.72	1.80
0	110	16.79	110	0.13	44	16.34	44	0.30	12.12	85	55	0.20	72	11.90	70	60	0.37	68	1.33	1.85
0.75	140	17.05	10	0.64	41	12.35	10	0.05	12.03	50	50	0.12	67	11.65	56	56	0.19	67	0.45	1.58
2	140	17.05	40	0.36	40	12.35	40	0.13	11.86	45	48	0.14	73	11.45	48	45	0.37	72	1.04	2.64
6	140	17.05	50	0.26	50	12.35	45	0.29	11.74	45	45	0.11	72	11.31	47	42	0.34	75	0.82	3.09
13	140	17.05	38	0.14	62	12.35	38	0.29	11.71	40	43	0.14	73	11.29	38	36	0.44	76	1.35	3.14
~45	140	17.05	54	0.05	65	12.35	54	0.42	11.63	40	40	0.13	73	11.20	34	32	0.40	72	1.13	3.08

T = 110 K, MA ⇌ MB $k_{12} = 65\ s^{-1}$. R: equivalents of methanol to Mannich base. I: signal intensities. W: signal linewidths in Hz. W_{DA1}/W_{DB1}: signal line widths of the low-field component of the doublet. W_{DA2}/W_{DB2}: signal linewidths of the high-field component of the doublet. M = monomer, MA = monomer A, MB = monomer B, D = dimer, DA = dimer A, DB = dimer B. $\delta^1H = {}^1H$ chemical shifts in ppm. $J(N,H) = {}^1J({}^1H,{}^{15}N)$.

MRC

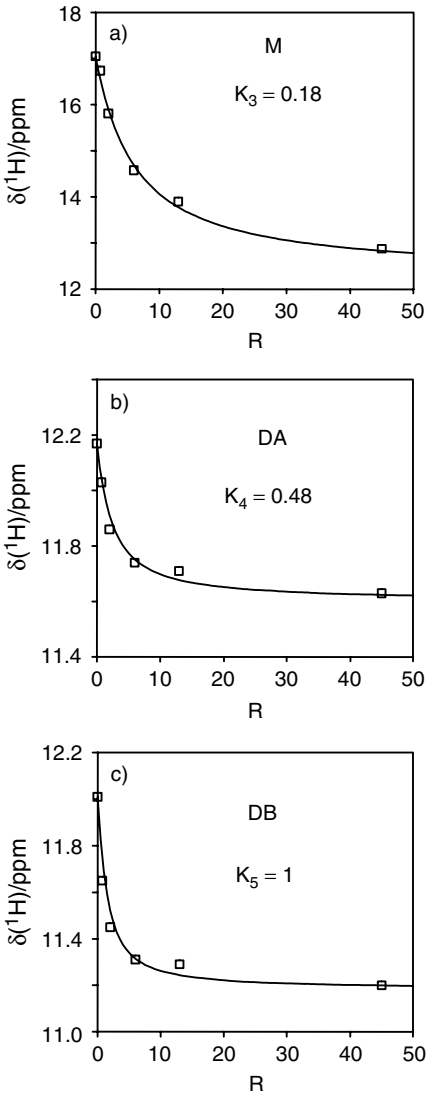

Figure 3. Fit of Eqn (7) to obtain the threshold value of the ^{1}H chemical shift for (a) the monomer–methanol complex AH···M, (b) AH···DA and (c) AH···DB.

Table 3. Rate constant $k_{21} = k_{12}(x_1/x_2)$ for the methanol solvation of the Mannich base Cl_3MB in CHF_3–$CHClF_2$ (2 : 1) as a function of temperature

R	$k'_f(s^{-1})$	x_1	x_2	$k_b(10^{-5}/s^{-1})$
0.75	1.1×10^6	0.64	0.05	140.80
2	1.1×10^6	0.36	0.13	30.46
6	1.1×10^6	0.26	0.29	9.86
13	1.1×10^6	0.14	0.29	5.31
45	1.1×10^6	0.05	0.42	1.31

R = equivalents of methanol to Mannich base; k'_f = pseudo-first-order rate constant for the 'desolvation process'' obtained from the simulation; x_1, x_2 = populations of the NMR signals corresponding to the unsolvated and solvated monomer; k_b = rate constant for the solvation of the monomer determined by simulation of the spectra given in Fig. 2(b)

The dimers exhibit a chemical shift of the hydrogen bond protons of 12 ppm and coupling constants $^1J(^1H, ^{15}N)$ of about 70 Hz. The latter values are close to the coupling constants found for protonated tertiary amines.[27] These findings support a zwitterionic hydrogen bond structure of the type $O^-\cdots H—N^+$ as indicated in Scheme 1 and show that the interpretation of the UV data in terms of a monomer–dimer equilibrium accompanied by a substantial proton dislocation from oxygen to nitrogen is correct.

These results could be obtained by NMR below 150 K, where the slow hydrogen bond exchange regime could be reached. If we had performed NMR experiments only at higher temperatures in the fast hydrogen bond exchange regime, various spectral changes could have been interpreted in terms of a classical proton transfer equilibrium between two forms. However, we would have missed the fact that in one form the molecule is monomeric and in the other dimeric. Naturally, there is no doubt that the dimerization is a true equilibrium, in contrast to proton transfer in the low-barrier hydrogen bond of the monomer.

As the chemical structures of the dimers DA and DB in Scheme 1(e) and (g) may not represent well the true conformations of these species, we tried to obtain more information about their structure by using DFT calculations at the B3LYP/6–31G** level on various monomeric and dimeric species using the Gaussian 94 program.[28] The calculated optimized gas-phase geometries are depicted in Fig. 4 and their quantitative characteristics are given in Table 4. Although the calculations do not refer to the polar solutions studied experimentally, they nevertheless show that the Mannich base studied does not form only monomers and dimers but that different substructures may occur exhibiting different conformations and hydrogen bond geometries.

Let us analyze first the results obtained for monomeric Cl_3MB for which three stationary conformations were found: an open structure (MO) where the hydrogen bond is broken and the OH group directed to the chlorine atom, and two conformers MA and MB exhibiting an intramolecular OHN hydrogen bond. MA and MB exhibit similar dipole moments of about 5 D, but differ in the CCOH and CCCN torsion angles. The conformation of MA is planar, i.e. the N, H and O atoms are located in the plane of the benzene ring, while the conformation of MB is bent, i.e. the chelate ring containing the O—H···N bridge does not lie in the plane of the benzene ring. The difference in the calculated energies of these conformers is small, i.e. 3.36 kJ mol^{-1}. The barrier between the conformers is also very small; no attempt was made to characterize the transition state of the interconversion. We tentatively assign MA and MB to the two signal components of M observed only at 110 K which coalesce into a single signal above this temperature, indicating a very fast conformeric exchange.

The comparison of the calculated energy of MO with those of MA and MB indicates that the O—H···N hydrogen bond in Cl_3MB is very strong, i.e. of the order of 50 kJ mol^{-1}. The calculations also showed that in the gas phase the zwitterionic forms of the monomers were not stable, as it was not possible to optimize their structures. However, this result does not mean that such polar states are not present in liquid Freons. Unfortunately, neither the calculations nor

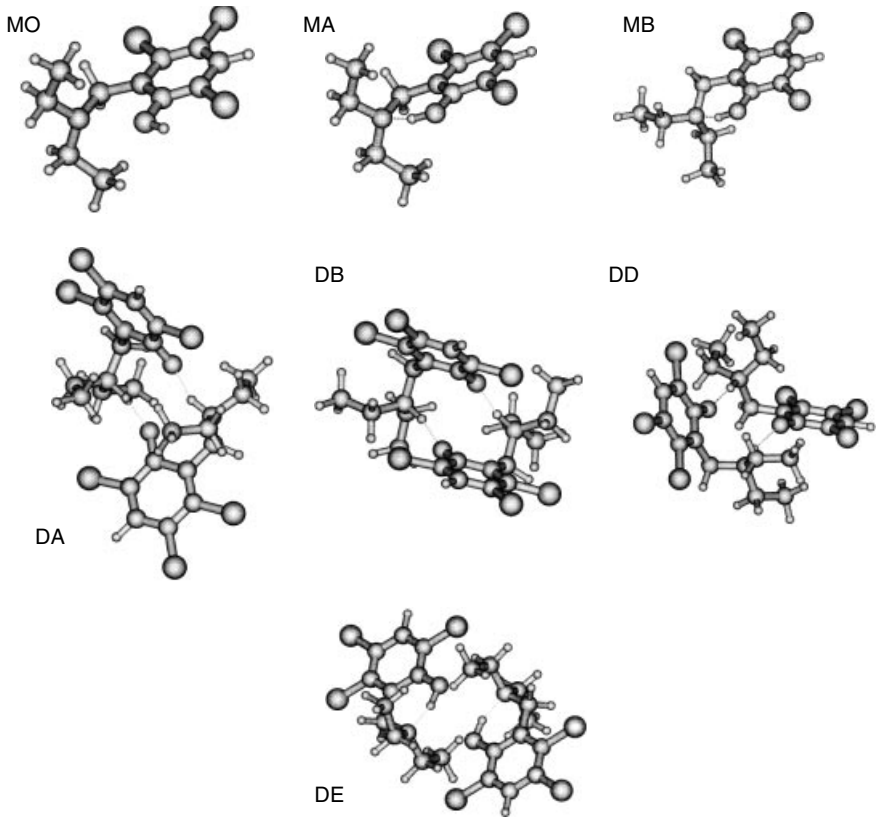

Figure 4. Optimized conformations of three monomeric species MO (open), MA and MB (hydrogen bonded) and four dimeric forms. DA and DB are zwitterionic and observed here by NMR. DD is also zwitterionic, but of lower stability. DE is centrosymmetric consisting of two planar MA monomers held together by van der Waals interactions.

Table 4. Calculated energies and structural parameters of the Mannich base Cl_3MB and its dimeric species defined in Fig. 4

Species	ΔE (kJ mol^{-1})	μ (D)	d (O···N) (Å)	d (O···H) (Å)	d (N···H) (Å)
MO	0	2.07	2.74	0.97	3.67
MA	−51.96[a]	5.19	2.56	1.01	1.58
MB	−55.22[a]	4.86	2.61	1.03	1.68
DA	+6.52[b]	3.22	2.66		1.06
DB	+5.98[b]	10.94	2.60		1.08
DD[c]	+26.95[b]	1.71	2.76		1.06
			2.59		1.06
DE	−23.95[b]	0	2.56	1.03	

[a] Compared with MO.
[b] Compared with MB.
[c] Two different N^+—H···O^- bridges.

the experiments performed in this study allow us to draw univocal conclusions about the hydrogen bond structures in the liquids used.

The most important results of calculations are related to the two dimeric conformations DA and DB. We assign these conformations to the two doublets in the ^{1}H NMR spectral region around 12 ppm (Fig. 2). Both conformers DA and DB exhibit even in the gas phase highly polar N^+—H···O^- hydrogen bonds. The less polar conformer DA exhibits an N···O distance of 2.66 Å and a dipole moment of $\mu = 3.22$ D. This structure is similar to that found by x-ray crystallography for 2-(*N*, *N*-diethylaminomethyl)-4-nitrophenol in the solid state.[29] The more polar conformer DB exibits a shorter O···N distance of 2.60 Å and a dipole moment of $\mu = 10.94$ D. Its geometry resembles that of 2-(*N*, *N*-dimethylaminomethyl)-3,4,5,6-tetrachlorophenol in the crystalline state.[3] The calculations show that the energy difference between DA and DB is only 0.54 kJ mol^{-1} in favor of conformer B. In both cases we find a small positive ΔE value for the dimerization. As the dimers are favored in the Freon solvents by lowering the temperature, this result indicates that the dimers are strongly stabilized by polar solvents owing to the reaction field effect and specific solvation.[30,31]

The calculations showed that in addition to the two most important DA and DB dimeric conformers, there are some other shallow minima corresponding to structure such as DD. Their appearance could be a reason of some disturbance of the doublet structure of signals at about 12 ppm. Moreover, one should mention that the optimization of the dimer DC with ionic bridges NHN^+ and OHO^- was not successful, probably for steric reasons.

Furthermore, the calculations indicate that two monomers can aggregate via van der Waals interactions leading to a fairly stable centrosymmetric dimeric form DE where the two monomeric units exhibit both two intramolecular hydrogen bonds (Table 4, Fig. 4). We expect the ^{1}H NMR chemical shift of DE also in the region of the monomeric forms around 17 ppm, and *a priori* it seems possible to assign one of the lines in this region to DE. However, we exclude

this interpretation based on the following argument. The dipole moment of DE is zero, in contrast to all other species. Thus, solute–solvent interactions of DE will be smaller than those of the other more polar species. As solvation implies a decrease in both enthalpy and entropy via solvent ordering, lowering the temperature will stabilize the polar species, and hence DE will not be observed in the case of the polar Freon solvent used in this study or of the polar and non-polar solvents of the previous molecular weight studies.[20]

Not only does the dimerization promote the proton dislocation from oxygen to nitrogen in the Mannich base studied, but also the addition of a proton donor such as methanol, as revealed by a high-field shift from 17 to 13 ppm for the hydrogen bond proton in monomeric Cl_3MB and to an increase in the coupling constant $^1J(^1H,^{15}N)$ from 40 to about 65 Hz. We assign this observation to the formation of a complex of the type AH···M as indicated in Scheme 1(d), where a negatively charged oxygen is stabilized by hydrogen bonding to methanol. This complex is in fast exchange with the non-solvated monomer; rate and equilibrium constants could be estimated, although the number of methanol molecules in the complex could not be determined. Therefore, the observed spectral changes arise most probably from the formation of additional hydrogen bonds to the oxygen atom, promoting a further charge separation, asymmetrization and, as a consequence, a weakening of the intramolecular hydrogen bond. Again, at present we are not able to judge whether the intramolecular hydrogen bond dynamics correspond to a proton transfer equilibrium between the tautomers of Scheme 1(a) and (c) or to a continuous dislocation of the single minimum from oxygen to nitrogen, starting from a non-polar towards a zwitterionic structure via a proton shared structure [Scheme 1(b)], as found recently in the case of the collidine–HF complex.[32]

The monomer/dimer ratio changes only slightly upon the addition of methanol, which is consistent with the above interpretation that the stabilization of both forms by methanol is similar. Generally, an increase in the solvent activity should favor more polar species. In fact, we observe a considerable influence of methanol added on the ratio between the two dimers DA and DB. The relative concentration of the dimer DB increases, which can be treated as evidence that this dimer corresponds to a more polar conformation more susceptible to the interaction with methanol molecules.

CONCLUSIONS

For the first time, using low-temperature ^1H NMR of the ^{15}N-labeled Mannich base Cl_3MB embedded in cold liquid Freons, we have shown that this molecule forms at low temperatures both monomers M and dimers D. In previous studies the sample temperatures were not low enough to achieve the slow exchange between monomers and dimers.[15–18]

The monomer M is characterized by a $^1H–^{15}N$ coupling constant of about 40 Hz, suggesting an equal sharing of the proton between oxygen and nitrogen. The potential for the proton motion is described in this case by either single broad minimum or double minimum with very low barrier and very short lifetimes of two limiting states. At very low temperatures, two conformers MA and MB could be observed which were assigned to different conformational states. DFT calculations for the isolated molecule indicated the formation of two conformers which differ slightly in energy, a planar conformation MA and a bent one MB, as depicted in Fig. 4.

Two different asymmetric dimers, DA and DB, were observed exhibiting slightly different zwitterionic $O^-\cdots H—N^+$ hydrogen bond geometries. Possible structures for these dimers are proposed, based on DFT calculations of the isolated complexes.

The increase in polarity of the solvent caused by adding methanol does not affect the monomer–dimer equilibria much but leads to a dramatic shift of the hydrogen bond protons towards nitrogen, as manifested in a decrease in their chemical shifts and an increase in the coupling constants $^1J(^1H,^{15}N)$. The effect is very strong for the monomers, but less pronounced for the dimers. The NMR signals indicate a fast dynamic process between the solvated and unsolvated forms.

We are aware that in the DFT calculations performed in this study the effects of the solvent were neglected, which provides a very crude approximation. Therefore, the numbers obtained cannot be directly compared with the experiment. We note, however, that calculations of chemical shifts together with the inclusion of solvent effects will allow a better comparison with theory and experiment in the future.

Acknowledgements

The financial support of the Deutsche Forschungsgemeinschaft, Bonn-Bad Godesberg, the Fonds der Chemischen Industrie, Frankfurt, and the Polish Committee for Scientific Research (Grant No. 09A03416) is gratefully acknowledged. The calculations were performed in the Wrocław Computer Center with the assistance of Mr J. Jañski.

REFERENCES

1. Sucharda-Sobczyk A, Sobczyk L. *Bull. Acad. Pol. Sci., Ser. Sci. Chim.* 1978; **26**: 549.
2. Koll A, Rospenk M, Sobczyk L. *J. Chem. Soc. Far 1* 1981; **77**: 2309.
3. Koll A, Wolschann P. *Monatsh. Chem.* 1996; **127**: 475.
4. Rutkowski K, Melikova SM, Koll A. *Vibr. Spectrosc.* 1994; **7**: 265; Rutkowski K, Koll A. *J. Mol. Struct.* 1994; **322**: 195.
5. Schreiber VM, Koll A, Sobczyk L. *Bull. Acad. Pol. Sci., Ser. Sci. Chim.* 1978; **26**: 651.
6. Koll A, Wolschann P. *Monatsh. Chem.* 1999; 130; 983.
7. Pawelka Z, Rospenk M, Sobczyk L. *Bull. Soc. Chim. Belg.* 1987; **96**: 615.
8. Rospenk M, Zeegers-Huyskens Th. *Spectrochim. Acta, Part A* 1986; **42**: 499.
9. Rospenk M. *J. Mol. Struct.* 1990; **221**: 109.
10. Filarowski A, Szemik-Hojniak A, Glowiak T, Koll A. *J. Mol. Struct.* 1997; **404**: 67.
11. Rospenk M, Zeegers-Huyskens T. *J. Phys. Chem.* 1987; **91**: 3974.
12. Rospenk M, Fritsch J, Zundel G. *J. Phys. Chem.* 1984; **88**: 321.
13. Filarowski A, Koll A. *Vibr. Spectrosc.* 1996; **12**: 15.
14. Rospenk M, Sobczyk L, Rabold A, Zundel G. *Spectrochim. Acta, Part A* 1999; **55**: 855.
15. Denisov GS, Gindin VA, Golubev NS, Koltsov AI, Smirnov SN, Rospenk M, Koll A, Sobczyk L. *Magn. Reson. Chem.* 1993; **31**: 1034.

16. Sitkowski J, Stefaniak L, Rospenk M, Sobczyk L, Webb GA. *J. Phys. Org. Chem.* 1995; **8**: 463.
17. Rospenk M, Sobczyk L. *Magn. Reson. Chem.* 1989; **27**: 445.
18. Rospenk M, Koll A, Sobczyk L. *Chem. Phys. Lett.* 1996; **261**: 283.
19. Koll A. *Bull. Soc. Chim. Belg.* 1983; **92**: 313.
20. Rospenk M, Koll A. *Pol. J. Chem.* 1993; **67**: 1851.
21. Golubev NS, Smirnov SN, Gindin VA, Denisov GS, Benedict H, Limbach HH. *J. Am. Chem. Soc.* 1994; **116**: 12055.
22. Smirnov SN, Golubev NS, Denisov GS, Benedict H, Schah-Mohammedi P, Limbach HH. *J. Am. Chem. Soc.*, 1996; **118**: 4094.
23. Shenderovich IG, BurtsevAP, Denisov GS, Golubev NS, Limbach HH. *Magn. Reson. Chem.* 2001; **39**: S91–S99.
24. Sucharda-Sobczyk A, Ritter S. *Pol. J. Chem.* 1978; **52**: 1555.
25. Siegel JS, Anet FAI. *J. Org. Chem.* 1988; **53**: 2629.
26. Ayllon J, Sabo-Etienne S, Chaudret B, Ulrich S, Limbach HH. *Inorg. Chim. Acta* 1997; **254**: 1.
27. Martin G, Martin ML, Gouesnard JP In *NMR-Basic Principles and Progress.* vol. 18, ^{15}N *NMR Spectroscopy.* Springer: Heidelberg, 1989.
28. Frisch MJ, Trucks GW, Schlegel HB, Gill PM, Johnson BG, Robb MA, Cheeseman JR, Keith T, Petersson GA, Montgomery JA, Raghavachari K, Al-Laham MA, Zakrzewski VG, Ortiz JV, Foresman JB, Cioslowski J, Stefanov BB, Nanayakkara A, Challacombe M, Peng CY, Ayala PY, Chen W, Wong MW, Andres JJ, Replogle ES, Gomperts R, Martin RL, Fox DJ, Binkley JS, Defrees DJ, Baker J, Stewart JP, Head-Gordon M, Gonzalez C, Pople JA. *Gaussian 94.* Gaussian: Pittsburgh, PA, 1995.
29. Filarowski A, Koll A, Glowiak T. *J. Chem. Crystallogr.* 1997; **27**: 707.
30. Bottcher CJF. *Theory of Electric Polarization*. Elsevier: New York, 1952.
31. Golubev NS, Denisov GS, Smirnov NS, Shchepkin DN, Limbach HH. *Z. Phys. Chem.* 1996; **196**: 73.
32. Golubev NS, Shenderovich IG, Smirnov SN, Denisov GS, Limbach HH. *Chem. Eur. J.* 1999; **5**: 492.